

# Fabrication of Gold Nanoparticles Using a Trithiol (Thiocyanuric Acid) as the Capping Agent

Yiwei Tan, Yongfang Li,\* and Daoben Zhu

Laboratory of Organic Solids, Center for Molecular Science,  
Institute of Chemistry, Chinese Academy of Sciences,  
Beijing 100080, People's Republic of China

Received October 29, 2001.

In Final Form: January 25, 2002

## Introduction

Synthesis of nanoparticles is an interesting field in solid-state chemistry.<sup>1</sup> The continuous interest in the design, synthesis, and characterization of nanosized metal particles has been driven by their unusual physical and chemical properties which are quite different from those of the bulk materials.<sup>2–5</sup> Intensive studies have been devoted to uses of metal nanoparticles as catalysts, ferrofluids, and sensors as well as their potential applications in a new generation of optical, electronic, and magnetic devices.<sup>2–6</sup>

The preparation of gold nanoparticles in aqueous systems has been extensively studied.<sup>6–10</sup> Recently, many synthetic schemes have been described for the production of gold particles in organic media.<sup>11–13</sup> One significant advance emerging from various synthetic strategies is the pioneering work of Brust, a two-phase chemical reduction route to nonaqueous transition metal particles bearing a surface coating of thiol.<sup>14</sup> The resultant nanoparticles have uniform size distribution and long-term stability in both solution and dry forms. This result is remarkable considering the inherent instability of metal and semiconductor nanoparticles due to aggregation and subsequent

precipitation from the suspension. In addition, the solution-phase reaction of Au nanoparticles with organic thiols leads to ease in self-assembly.

The preparation of stable noble metallic colloids based on a strong affinity of sulfur to the surfaces of metal particles has received extensive attention. So far, many sulfur-containing molecules, including alkanethiols (dithiols), disulfides,<sup>15</sup> episulfide,<sup>16</sup> alkylthiosulfate,<sup>17</sup> xanthates,<sup>18</sup> and carbon disulfate,<sup>19</sup> have been used to generate self-assembled monolayers on metallic nanoparticles (Ag, Au, Pt, etc.). However, it is still desirable to develop new types of capping agents for the synthesis of stable nanoparticles with desired shape and size. In this paper, we use a capping agent, a star-shaped trithiol molecule (thiocyanuric acid (TCA)) rather than extended long-chain thiols, to prepare Au nanoparticles with controlled size and morphology.

## Experimental Section

**Materials and Instrumentation.** Hydrogen tetrachloroaurate(III) and tetraheptylammonium bromide were purchased from Aldrich. TCA purchased from TCI (Tokyo) was vacuum-dried at 60 °C for 24 h and stored in a vacuum desiccator before use. Potassium bitartrate, sodium borohydride, and tetrahydrofuran (THF) were supplied by Beijing Chemical Reagent Co. All chemicals were used without further purification. The water used throughout this work was degassed high-purity water processed by distillation of deionized water.

**TEM Observations and EDS Measurements.** A JEOL-JEM-200 CX and a JEOL-JEM-2010F transmission electron microscope (TEM), operated at 200 kV, were employed to size and analyze the particles for different purposes. Energy-dispersive X-ray spectroscopy (EDS) analysis was performed on the JEOL-JEM-2010 transmission electron microscope which was equipped with a nanoarea energy-dispersive X-ray spectroscopic analyzer. Selected area electron diffraction (SAED) data were acquired with the JEOL-JEM-200 CX transmission electron microscope. TEM specimens were prepared by placing a drop of a gold nanoparticle solution on an amorphous carbon-coated copper microgrid and allowing the solvent to slowly evaporate in air. Diffraction patterns were obtained at a camera length of 70 cm.

**XPS Measurements.** X-ray photoelectron spectroscopy (XPS) data were obtained on a VG-Scientific ESCA Lab 220i-XL spectrometer equipped with a hemisphere analyzer, a multi-channel detector, a toroidal monochromator, and an Al K $\alpha$  X-ray source at 1486.6 eV. The precipitated Au nanoclusters were washed in turn with heated ionized water (80 °C) and THF several times to remove unbound sulfur-containing species and carboxylates and then completely dried under vacuum at 80 °C. Peak positions were internally referenced to the C1s peak at 284.6 eV.

**Synthesis. Direct Chemical Reduction.** Gold particles were prepared with potassium bitartrate as the reductant. Typically, the molar ratio of TCA to HAuCl<sub>4</sub> was fixed at 1:1.

A 25 mL sample of 1.0% (wt %) aqueous potassium bitartrate solution was prepared in a 100 mL round-bottom flask. The solution was brought to boiling while stirring, and the TCA–Au polymer solution prepared by mixing 25 mL of an aqueous HAuCl<sub>4</sub> solution (0.001 M) with 0.25 mL of a TCA solution in THF (0.10 M) was added quickly.<sup>20</sup> The solution turned wine red after 30

\* To whom correspondence should be addressed. Fax: 86-10-62559373. E-mail: liyf@infoc3.icas.ac.cn.

- (1) Ozin, G. A. *Adv. Mater.* **1992**, *4*, 612.
- (2) (a) Lu, L.; Sui, M. L.; Lu, K. *Science* **2000**, *287*, 1463. (b) Collier, C. P.; Saykally, R. J.; Shiang, J. J.; Henrichs, S. E.; Heath, J. R. *Science* **1997**, *277*, 1978.
- (3) (a) Siegel, R. *Nanostruct. Mater.* **1993**, *3*, 1. (b) Ayappan, S.; Gopalan, R. S.; Subbana, G. N.; Rao, C. N. R. *J. Mater. Res.* **1997**, *12*, 398.
- (4) (a) Henglein, A. *Chem. Rev.* **1989**, *89*, 1861. (b) Lewis, L. N. *Chem. Rev.* **1993**, *93*, 2693. (c) Oggawa, S.; Hayashi, Y.; Kobayashi, N.; Tokizaki, T.; Nakamura, A. *Jpn. J. Appl. Phys.* **1994**, *33*, L331.
- (5) (a) *Clusters and Colloids*; Schmid, G., Ed.; VCH: Weinheim, 1994. (b) Alivisatos, A. P. *Science* **1996**, *271*, 933 and references therein. (c) Colvin, V. L.; Schlamp, M. C.; Alivisatos, A. P. *Nature* **1994**, *370*, 354.
- (6) Turkevich, J.; Stevenson, P. C.; Hillier, J. *Discuss. Faraday Soc.* **1951**, *11*, 55.
- (7) (a) Brown, K. R.; Walter, D. G.; Natan, M. J. *Chem. Mater.* **2000**, *12*, 306. (b) Brown, K. R.; Lyon, L. A.; Fox, A. P.; Reiss, B. D.; Natan, M. J. *Chem. Mater.* **2000**, *12*, 314. (c) Jana, N. R.; Gearheart, L.; Murphy, C. J. *Chem. Mater.* **2001**, *13*, 2313.
- (8) (a) Frens, G. *Nature* **1973**, *241*, 20. (b) Siiman, O.; Hsu, W. P. *J. Chem. Soc., Faraday Trans. 1* **1986**, *82*, 851.
- (9) (a) Yu, Y. Y.; Chang, S. S.; Lee, C. L.; Wang, C. R. C. *J. Phys. Chem. B* **1997**, *101*, 6661. (b) Chang, S. S.; Shih, C. W.; Chen, C. D.; Lai, W. C.; Wang, C. R. C. *Langmuir* **1999**, *15*, 701.
- (10) (a) Henglein, A. *Langmuir* **1999**, *15*, 6738. (b) Chen, S. W. *Langmuir* **1999**, *15*, 7551.
- (11) (a) Han, M. Y.; Quek, C. H. *Langmuir* **2000**, *16*, 362. (b) Han, M. Y.; Quek, C. H.; Huang, W.; Chew, C. H.; Gan, L. M. *Chem. Mater.* **1999**, *11*, 1144.
- (12) (a) Yee, C. K.; Jordan, R.; Ulman, A.; White, H.; King, A.; Rafailovich, M.; Sokolov, J. *Langmuir* **1999**, *15*, 3489. (b) Quinn, M.; Mills, G. J. *Phys. Chem.* **1994**, *98*, 9840.
- (13) Green, M.; O'Brien, P. *Chem. Commun.* **2000**, 183.
- (14) Brust, M.; Walker, M.; Bethell, D.; Schiffrin, D. J.; Whyman, R. *J. Chem. Soc., Chem. Commun.* **1994**, 801.

- (15) (a) Poter, L. A., Jr.; Ji, D.; Westcott, S. L.; Graupe, M.; Czernuszewicz, R. S.; Halas, N. J.; Lee, T. R. *Langmuir* **1998**, *14*, 7378.
- (16) Suzuki, M.; Miyazaki, T.; Hisamitsu, H.; Kadoma, Y.; Morioka, Y. *Langmuir* **1999**, *15*, 7409.
- (17) Shon, Y. S.; Gross, S. M.; Dawson, B.; Porter, M.; Murray, R. W. *Langmuir* **2000**, *16*, 6555.
- (18) Sawant, P.; Kovalev, E.; Klug, J. T.; Efrima, S. *Langmuir* **2001**, *17*, 2913.
- (19) Jiang, X.; Xie, Y.; Lu, J.; Zhu, L.; He, W.; Qian, Y. *Langmuir* **2001**, *17*, 3795.

s, indicating the production of Au nanoparticles. The boiling and stirring were continued for ca. 2 min, and then the solution was cooled to room temperature immediately in a cold water bath. A control system was also prepared with the same protocol but in the absence of TCA. Upon addition of  $\text{HAuCl}_4$ , the color of the solution underwent a series of variations, that is, changed first from light yellow to blue-gray (after ca. 1 min) as the Au nanoparticles formed and subsequently to orange (after ca. 5 min) when the Au nanoparticles agglomerated and precipitated from the suspension. Following each synthesis, a drop of the Au sol was left on a copper grid for TEM measurements.

**Ligand Exchange Reaction.** Stable solutions of Au nanoparticles in toluene were prepared following a method similar to that described by Brust and co-workers.<sup>14</sup> The as-prepared nanocrystals were then coated with TCA through ligand exchange. A total of 30.6 mg of  $\text{HAuCl}_4$  was dissolved by sonication in 25 mL of a 0.0158 M solution of tetraheptylammonium bromide (THAB) in toluene. The toluene solution had been bubbled with dry  $\text{N}_2$  gas for 1 h and then was mixed fully with 5 mL of a freshly prepared 0.102 M aqueous  $\text{NaBH}_4$  solution under vigorous stirring for 20 min. The yellow organic phase immediately turned wine red for the production of gold colloid. The colloid was cooled to ca. 0 °C and aged for 4 weeks. A total of 10 mL of the top layer of the as-prepared Au nanocrystal solution in toluene was withdrawn and then annealed at 110 °C under reduced pressure for ca. 1.5 h. After this heating treatment, the color of the solution changed from wine red to pinkish. Finally, the Au colloids were coated with TCA through ligand exchange. An excess of TCA solution in THF (0.4 mL, 0.27 M) was added to the gold colloid to ligate the nanoparticle surfaces. The particles react readily with TCA, as manifested by giving a dark-gray solution within a few seconds. The colloid was preserved at ca. 0 °C for ca. 2 h. Each 0.1 mL of the top layer of gold nanocrystal colloid was deposited in a different volume of pure toluene to obtain a desired nanocrystal concentration. A 10  $\mu\text{L}$  sample of each solution was dropcasted on a copper grid for TEM measurements.

## Results and Discussion

**Sizes and Structures of Au Nanoparticles Prepared with Potassium Bitartrate as the Reductant.** Au colloids obtained by reduction of  $\text{HAuCl}_4$  with potassium bitartrate without the addition of TCA are used as the control system. These Au colloids are unstable because potassium bitartrate and its corresponding oxidation products are not effective in stabilizing gold nanoparticles. Figure 1a illustrates a representative TEM micrograph where the "unprotected" Au nanoparticles aggregate and display spherical, triangular, and hexagonal outlines with a mean diameter of ca. 60 nm. Rod shapes are also observed in the TEM images. The length of each "rod" is almost equal to the distance between the opposite corners of the hexagonal particles. Those rodlike particles are the erect hexagonal Au nanoparticles (in a sidewise orientation on the TEM grid), which demonstrates that the platelet Au particles have a thickness of about 20 nm as judged from the traverse diameters of the rods. A similar case for gibbsite ( $\text{Al}(\text{OH})_3$ ) is described by Lekkerkerker et al. recently.<sup>21</sup> When TCA–Au polymer is used as the precursor,

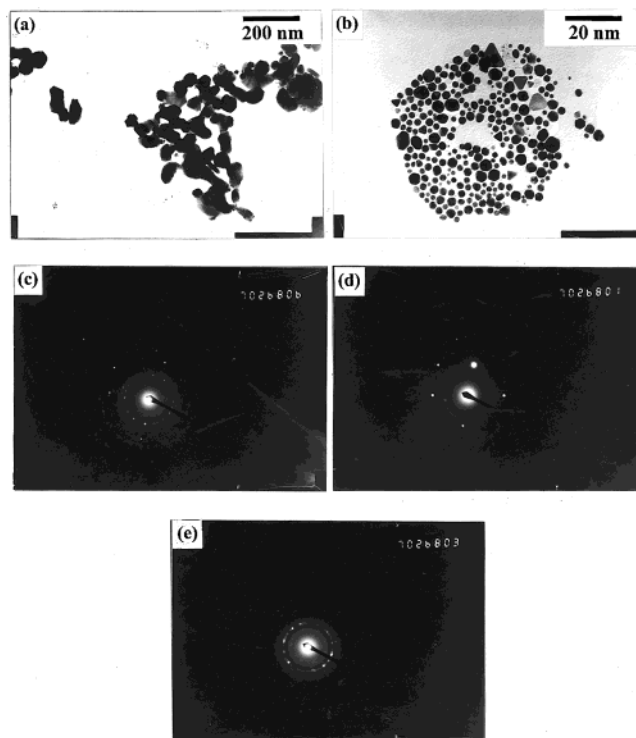


**Figure 1.** Electron microscopic images of the as-prepared Au nanoparticles synthesized under reflux with potassium bitartrate as the reductant: (a) without addition of TCA and (b) in the presence of TCA. The corresponding ED patterns for (c) the triangular, (d) the square, and (e) the hexagonal Au nanoparticles. Experimental conditions:  $\text{HAuCl}_4$ : 25 mL, 0.001 M; TCA: 0.25 mL, 0.10 M; potassium bitartrate: 25 mL, 1.0% (wt %). The mole ratio of  $\text{HAuCl}_4$ /TCA is 1:1.

the obtained Au colloids have a long-term stability. No precipitation of Au nanoparticles takes place after a few days. Figure 1b shows a typical TEM image of the TCA–Au nanoparticles. The morphology and dimension of Au particles are significantly different from the control system shown in Figure 1a; moreover, the number of shaped Au nanoparticles remarkably increases. The Au nanoparticles exhibit triangular, square, and hexagonal shapes besides round and irregular shapes. In addition, some pentagonal particles can also be identified in TEM images. However, there are no such nanoparticles in the TEM images of the control system. Accordingly, these two-dimensional shapes may correspond for example to tetrahedrons, cubes, icosahedrons, polyhedrons, small bodies, and decahedrons, respectively.<sup>22,23</sup> These faceted or rodlike particles are occasionally observed for weak reducing agents where growth occurs over a longer period.<sup>24</sup> El-Sayed et al. provided two reasonable explanations for the formation of faceted and rod-shaped particles: (i) the growth rates vary at different planes of the particles and (ii) particle growth competes with the capping action of stabilizers (in our case TCA).<sup>25</sup> In our case, one possible mechanism for the formation of various shaped Au nanoparticles is that potassium bitartrate is a relatively "slow" reducing agent. Therefore, there is enough time for the reduction of TCA–Au polymer into elemental Au, which then agglomerates and grows into Au nanoparticles with a more regular shape. Meanwhile,

(20) (a) The  $[\text{AuCl}_4]^-$  solution lost its yellow color gradually upon mixing with TCA and turned a red-brown color due to the formation of a TCA–Au polymer. Although the exact structure of the TCA–Au polymer is unknown presently, a TCA-induced reduction of  $\text{Au}(\text{III})$  to  $\text{Au}(\text{I})$  occurs, which is verified by the XPS measurements of the product obtained by mixing TCA with  $\text{HAuCl}_4$  at a molar ratio of 1:1 (TCA/ $\text{AuCl}_4^-$ ). The peak positions of  $\text{Au}4f$  and  $\text{S}2p$  appear at 84.5 and 163.4 eV, respectively. These values are close to the document data for  $\text{Au}(\text{I})$  compounds and disulfides. (b) Similar results are found in the literature such as: (i) Alvarez, M. M.; Khoury, J. T.; Schaaff, T. G.; Shafgullin, M.; Vezmar, I.; Whetten, R. L. *Chem. Phys. Lett.* **1997**, *266*, 91. (ii) Hostetler, M. J.; Wingate, J. E.; Zhong, C.-J.; Harris, J. E.; Vachet, R. W.; Clark, M. R.; London, J. D.; Green, S. J.; Stokes, J. J.; Wignall, G. D.; Glish, G. L.; Porter, M. D.; Evans, N. D.; Murray, R. W. *Langmuir* **1998**, *14*, 17.

(21) van der Kooij, F. M.; van der Beek, D.; Lekkerkerker, H. M. W. *J. Phys. Chem. B* **2001**, *105*, 1696.

(22) Harfenist, S. A.; Wang, Z. L.; Whetten, R. L.; Vezmar, I.; Alvarez, M. M. *Adv. Mater.* **1997**, *9*, 817.

(23) Wang, Z. L. *Adv. Mater.* **1998**, *10*, 13.

(24) Goia, D. V.; Matijevic, E. *New J. Chem.* **1998**, *22*, 1203.

(25) Petroski, J. M.; Wang, Z. L.; Green, T. C.; El-Sayed, M. A. *J. Phys. Chem. B* **1998**, *102*, 3316.

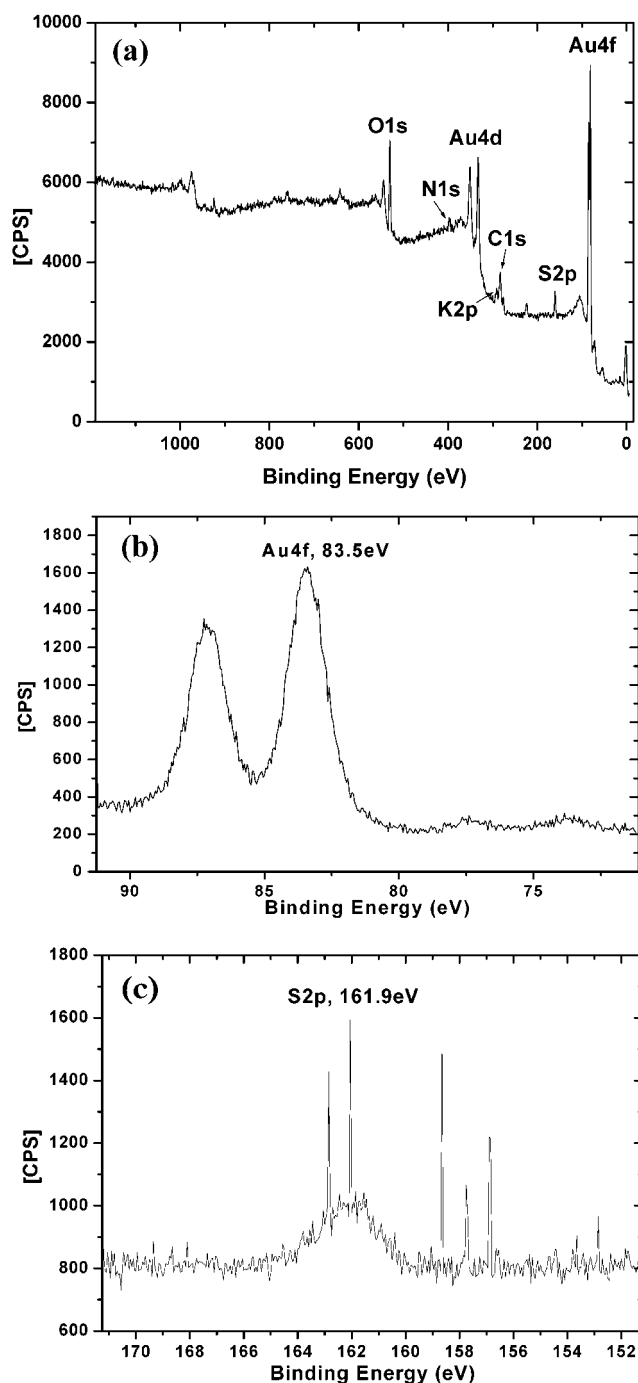


**Figure 2.** XPS spectra of the products obtained from reducing the TCA-Au polymer precursor by potassium bitartrate: (a) XPS survey spectrum of gold, (b) binding energy spectrum for Au4f, and (c) binding energy spectrum for S2p.

the growth is suppressed at some faces of Au particles as a result of capping by TCA but takes place at other faces. The diameter of Au particles notably decreases to the range of 5–20 nm. The capping agent has an important influence on the size and morphology of the Au nanoparticles. The electron diffraction patterns for triangular, square, and hexagonal particles are presented in Figure 1c–e. The discrete diffraction spots illustrate the crystalline features of the shaped Au nanoparticles.

To determine the components, the Au nanoparticles are subject to XPS measurements and EDS analysis. From the XPS spectra (Figure 2a) comes the XPS survey spectrum of Au atoms. The appearance of S, O, and K peaks in the XPS data reveals that not only sulfur-

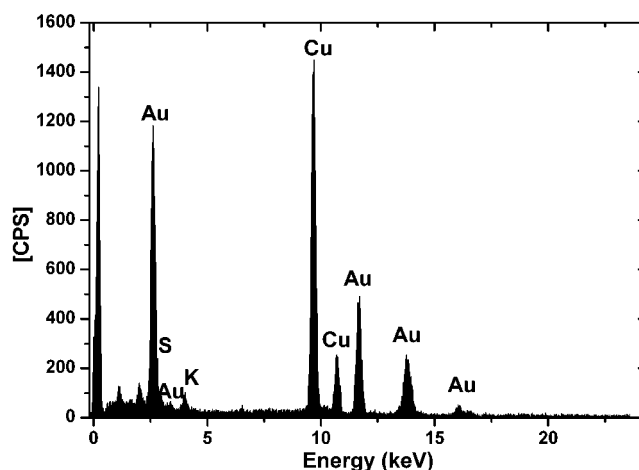


**Figure 3.** EDS analysis of a randomly selected Au nanoparticle prepared by reducing the TCA-Au polymer using potassium bitartrate as the reductant.

containing species but also carboxylates adsorb onto the Au nanoparticles. As expected, the binding energy of 83.5 eV for Au4f is similar to that of pure Au (84.0 eV)<sup>26</sup> (see Figure 2b). Figure 2c shows a characteristic peak of S2p at a binding energy of 161.9 eV belonging to metal sulfide, which suggests the formation of a S–Au bond. The identification of the product was also confirmed by EDS as shown in Figure 3. A randomly selected nanoparticle on the copper grid is analyzed. In the EDS spectrum, the K and S signals are present besides the Au signal, indicating the adsorption of sulfur-containing species and carboxylates on the Au particle core surfaces. This result is in good agreement with XPS measurements. The atomic ratio of Au/K/S is ca. 82/5/13.

**TCA-Mediated Aggregation of Gold Nanoparticles after Ligand Exchange.** It was discovered that aging the nanoparticle solution often leads to low size dispersity. Significant sample aging takes weeks or months. In analogy to the previous experimental results,<sup>27</sup> we have also shown that the size distribution of nanocrystals can be considerably narrowed after being refluxed with THAB ligand. Further size segregation occurs after lowering the Au colloid temperature. As a result, the top layer of the gold colloid becomes highly monodisperse, in which more than 80% of the population is within the range of 6–8 nm.

The cross-linkage of TCA finally results in an insoluble precipitate. Therefore, ordered structures are observed by TEM in the early stage of the self-assembly process. Figure 4 presents three pairs of representative micrographs of Au nanoparticle array patterns on carbon films of copper grids before and after ligand exchange. A series of distinguishable gold nanoparticle films are observed after evaporation of the gold colloids with various particle concentrations in toluene. As we increase the concentration of THAB-encapsulated Au nanoparticles, the packing morphology varies from scattered Au nanoparticles to isolated domain structures and ultimately to percolating domains. One can see that scattered and randomly arrayed Au nanoparticles aggregate and self-organize into hexagonal arrays with increasing particle concentration. Such changes in nanoparticle film structures have already been reported in the literature.<sup>28,29</sup> Deegan et al. proposed a

(26) Hüfner, S. *Photoelectron Spectroscopy*, 2nd ed.; Springer-Verlag: New York, 1996.

(27) Zhong, C. J.; Zhang, W. F.; Leibowitz, F. L.; Eichelberger, H. H. *Chem. Commun.* **1999**, 1211.

(28) For example: (a) Yin, J. S.; Wang, Z. L. *Phys. Rev. Lett.* **1997**, 79, 2570. (b) Giersig, M.; Mulvaney, P. *Langmuir* **1993**, 9, 3408.



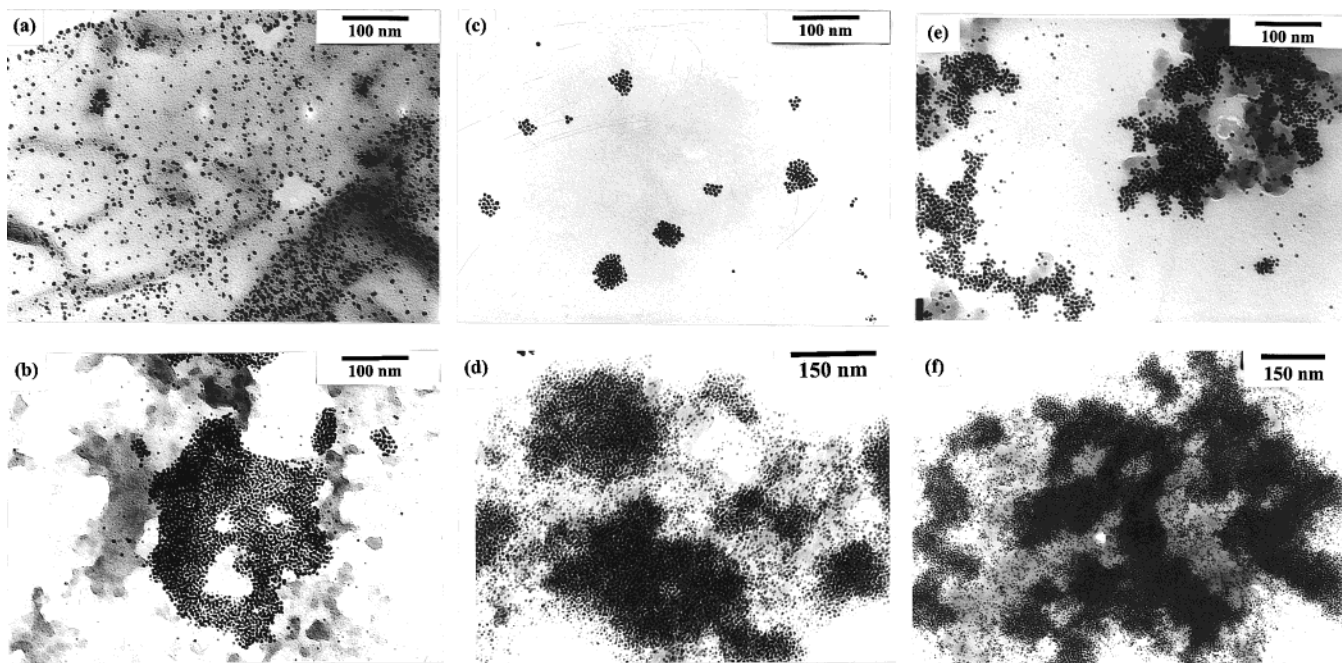


**Figure 4.** Nanocrystal patterns formed by depositing 10  $\mu\text{L}$  of gold nanocrystal colloid in toluene encapsulated by THAB ((a), (c), and (e) on the top) and following ligand exchange using TCA ((b), (d), and (f) on the bottom) with various particle concentrations:  $2.5 \times 10^{11} \text{ mL}^{-1}$  for (a) and (b),  $1.0 \times 10^{12} \text{ mL}^{-1}$  for (c) and (d), and  $4.6 \times 10^{12} \text{ mL}^{-1}$  for (e) and (f).

mechanism for the changes in film structure.<sup>30</sup> Bilayer or multilayer films containing hexagonally organized Au nanocrystals appear on carbon film substrates through ligand exchange, even at very low concentrations of Au nanocrystals. The packing is facilitated in many places by a curved arrangement of the nanocrystals, probably due to the triangular linkage of TSA. By comparing part a with part b, part c with part d, and part e with part f in Figure 4, we find that the formation of compacted multilayers is almost independent of nanoparticle concentration. Interparticle interaction becomes so strong for the displacement reaction of TCA on the surfaces of Au nanoparticles that these superlattices may be too tough to be perturbed when dewetting finally takes place. Since the size of the particles is in a rather broad range of 5–8 nm, the hexagonal packing is imperfect in places. In Figure 4b, three different regions can be observed, corresponding to monolayers, partial bilayers, and trilayers of Au nanocrystals. At higher concentrations of Au nanoparticles, only bilayer and multilayer nanoparticulate films are obtained, as demonstrated in Figure 4d,f. The TEM images also show that the scattered nanoparticles do not coalesce to larger units. The absence of S signal appearance in the EDS of the isolated particles suggests that the capping layers of these particles are not fully replaced with TCA. The pattern of overlapping two layers of Au nanoparticles is the ring structure as reported by Schiffrin et al.,<sup>31</sup> where the nanocrystals in the top layer occupy 2-fold saddle sites to form hexagonal rings which are rotated by  $30^\circ$  relative to the lower layer. The 2-fold site occupancy may be originated from one S atom of TCA adsorbed on a particle in the top layer and two other S atoms anchored on two neighboring particles in the lower layer.

Although such self-organized multilayer films of metal nanocrystals have been investigated prior to this work,<sup>31,32</sup> there are unique features in our system. First, the self-organized structures of TCA-derivatized Au nanoparticles are tenacious because the interparticle chemical bond is present, which is much stronger than the weak van der Waals interaction observed in those previously described systems. Second, the nanoparticles can self-organize to both 2D and 3D arrays (bilayers and trilayers or multilayers of nanoparticle films) due to the three mercapto groups in TCA. Finally, the 3D arrays can form at a rather lower concentration of Au nanoparticles than that reported in ref 31 due to the TCA linkage.

In summary, the aqueous Au colloid solution prepared by directly reducing gold ions with potassium bitartrate is unstable in the absence of TCA. TEM micrographs show aggregated large spherical, triangular, and hexagonal Au nanoparticles with a mean size of ca. 60 nm. However, after reduction of the TCA–Au polymer precursor using potassium bitartrate as the reductant, homogeneously distributed Au nanoparticles are observed in TEM images where a large number of well-defined faceted nanocrystals are found in varied geometric shapes. The TCA–Au nanocrystals demonstrate a narrow size distribution. Our studies also reveal that following place exchange reaction on the surfaces of Au nanoparticles by TCA, Au nanoparticles can form 2D and 3D arrays even at a very low concentration due to the trithiol (TCA) cross-linkages, where each top layer Au nanoparticle occupies a 2-fold saddle site between two Au particles in the lower layer.

**Acknowledgment.** This work was supported by The Chinese Academy of Sciences. We thank Dr. Liu Fen for help with the XPS experiments.

LA011612F

(29) (a) Taleb, A.; Petit, C.; Pileni, M. P. *Chem. Mater.* **1997**, *9*, 950. (b) Motte, L.; Billoudet, F.; Cacaze, E.; Douin, J.; Pileni, M. P. *J. Phys. Chem. B* **1997**, *101*, 138. (c) Motte, L.; Pileni, M. P. *J. Phys. Chem. B* **1998**, *102*, 4014. (d) Pileni, M. P. *J. Phys. Chem. B* **2001**, *105*, 3358.

(30) Deegan, R. D.; Bakajin, O.; Dupont, T. F.; Huber, G.; Nagel, S. R.; Witten, T. A. *Nature* **1997**, *389*, 827.

(31) Fink, J.; Kiely, C. J.; Bethell, D.; Schiffrin, D. J. *Chem. Mater.* **1998**, *10*, 922.

(32) (a) Lim, M. H.; Ast, D. G. *Adv. Mater.* **2001**, *13*, 718. (b) Zanchet, D.; Moreno, M. S.; Ugarte, D. *Phys. Rev. Lett.* **1999**, *82*, 5277. (c) Heath, J. R.; Knobler, C. M.; Veff, D. V. *J. Phys. Chem. B* **1997**, *101*, 189.